PNAS

Supporting Information for

Mechanical stress during confined migration causes aberrant mitoses and c-MYC amplification

Giulia Bastianello[1,2,6*], Gururaj Rao Kidiyoor[1,3,6], Conor Lowndes[1], Qingsen Li[1], Raoul Bonnal[1], Jeffrey Godwin[1], Fabio Iannelli[1], Lorenzo Drufuca[2], Ramona Bason[1], Fabrizio Orsenigo[1], Dario Parazzoli[1], Mattia Pavani[1], Valeria Cancila[4], Stefano Piccolo[1,5], Giorgio Scita[1,2], Andrea Ciliberto[1], Claudio Tripodo[1,5], Massimiliano Pagani[1-2] and Marco Foiani[1,2*].

* Corresponding author. Giulia Bastianello[1,2,6*], Marco Foiani[1,2*].

Email: giulia.bastianello@ifom.eu; marco.foiani@ifom.eu.

This PDF file includes:

S1. Materials and Methods

S1.1 Cell lines and reagents.

Cell lines.

HeLa cells with stable H2B-mCherry expression were already described (20). U2OS-FUCCI cells were from Libor Macůrek (45). U2OS-Cyclin B1-eYFP stable cell line was from (49). Stable U2OS expressing Tubulin-mCherry and H2B-GFP were from Andrea Ciliberto lab.

Antibodies and reagents.

Rabbit monoclonal anti-c-Myc ab32072 was used for IHC to stain c-MYC protein in metastatic tissues.

Reversine 0.5 μM (R3904, Sigma) was used to inhibit the mitotic Spindle Assembly Checkpoint. Nocodazole (M1404, Sigma) at increasing concentrations was used to arrest U2OS cells in mitosis. To perform drug treatments in micro-channel devices, cells were incubated with the drugs 1h before trypsinization and loading, drugs were maintained in media inside the micro-channels for the entire experiment. DMSO was used in control samples at the same concentration.

S1.2 PDMS channels preparation.

A mixture 1:9 of polymer and crosslinking agent (RTV615 kit) was poured in the silicon mold until complete polymeriation. PDMS channels were bound on 2 chambers Lab-TeK II 155379 glasses (Thermofisher) or Nunc™ Glass base dishes (150682, Thermofisher) using plasma treater. Channels were fibronectin coated overnight, washed with PBS, and filled with cell culture medium for one day (adding treatments or inhibitors when needed).

S1.3 Imaging analysis of cells undergoing confined migration.

Nuclear speed analysis across constrictions was done manually counting the number of frames required for a nucleus to migrate across the pore, only nuclei that performed a complete passage during the time-lapse were considered for the analysis.

Movies of U2OS tubulin-mCherry H2B-GFP were manually analyzed to score defective mitoses during migration in micro-channels. Mitoses showing disorganized mitotic spindle with unequal distribution of sister chromatids and resulting in daughter cells with significant nuclear size difference were counted as defective mitosis.

The manual analysis of CyclinB1 fluctuations at G2-M transition in migrating cells was performed counting the time frames occurring between the accumulation of CyclinB1 (late G2), the nuclear internalization of cyclinB1 (Metaphase) and the complete degradation of Cyclin B1 (end of mitosis). Fluorescence intensity quantifications of eYFP-CyclinB1 during migration were performed using Fiji by measuring the average projection of the signal on a circular ROI designed inside the cell boundary.

S1.4 Imaging analysis of CyclinB1 degradation following Nocodazole

Images were acquired on a DeltaVision Elite system (GE Healthcare) using 60x immersion objective (Olimpus) and a CoolSNAP HQ CCD camera. Temperature of 37°C and 5%CO2 were maintained with Okolab incubator. For each position, 3 z stacks 6 μm apart were acquired for 48h every 6 minutes and images were analyzed using Fiji software. eYFP-CyclinB1 intensities were quantified from accumulation (late G2) to mitotic exit. Nuclear

Envelope Break Down (NEBD) and cell re-adhesion were used as mitotic entry and exit markers. Both of them were visually assessed on DIC images.

The analysis was performed using Fiji, fluorescence intensity was measured designing a circular ROI inside the cell boundary on the average projection.

S1.5 Cell seeding in micro-channel device for scRNA-sequencing.

PDMS devices mounted on bottom slide-glasses were coated with fibronectin 20μg/ml overnight, washed three times with PBS sterile and incubated with cell culture media overnight.

For these experiments 0.2μm-filtered cell culture media was used in order to remove debris that could affect single cell sequencing protocol.

Cell seeding into the device was performed 72h before collection. Before cell seeding, cell culture media was removed in both seeding and collection chambers. This facilitate the cell seeding procedure as cell suspension is loaded only in the central chamber and the chambers are communicating vessels. Single clone-derived U2OS cells were used for this experiment, for all experiments, cells were thawed one week before seeding inside the device, cells were split one to four and then 1 to six over the one-week culture time.

U2OS cells were counted and resuspended at a final concentration of 10^6 cells/ml, using a p20 pipette, cells were loaded in the central chamber of the device filling completely the chamber volume and allowing cell suspension to reach the entrance of the channels immediately after cell seeding. Cell culture media was added in the collection chambers and devices were incubated at 37˚C inside 15cm Petri dishes. Cells were allowed to migrate inside the devices for 72h and cell culture media was changed every day in seeding and

collection chamber.

S1.6 Sequencing library construction using the Chromium 10X platform.

Single cell suspensions of U2OS cells migrated across straight or constriction channels were loaded on a Chromium 10X Instrument (10x Genomics) to generate single-cell GEMs. Following mRNA capture and reverse transcription, GEMs were broken and the single-strand cDNA was cleaned up and amplified by PCR following the manufacturer instructions. Single-cell RNA-seq libraries were prepared from cDNA using Chromium™ Single Cell 3' Library Construction Kit. Sequencing libraries were loaded on an Illumina Novaseq platform and sequenced at 50000 reads per cell for gene expression analysis.

S1.7 scRNA-seq data processing and quality control.

The FASTQ files of XXX cells were processed by the Cell Ranger software pipeline v6.1.2 provided by 10x Genomics using default parameters, creating a raw count matrix for each analyzed sample. Each matrix was then processed using the Python package Scanpy v1.8.2 (95). First, cells with fewer than 200 expressed genes and genes detected in less than 0.1% of the total sample cells and cells with fewer than 200 expressed genes were removed. Low-quality cells and outliers based on the percentage of mitochondrial and ribosomal genes, total number of genes and gene counts were detected according to the median absolute deviation (MAD). Cells were removed if the value of any of the above features was greater than the number of selected MAD above the median. After filtering, matrices were then normalized using a scaling factor of 1e4 and log-transformed using scanpy.pp.normalize_per_cell(data, counts_per_cell_after = 1e4) and

scanpy.pp.log1p(data), respectively. Hghly variable genes (HVGs) were selected based on specific thresholds for mean expression and dispersion using scanpy.pp.highly_variable_genes(min_mean = 0.2, max_mean = 3, min_disp = 0.5) and excluding mitochondrial and ribosomal genes.

Dimensionality reduction and clustering.

Principal component analysis was performed on scaled and centered values considering selected HVGs. Unwanted sources of variation (that is, number of detected counts and genes per cell, percentages of mitochondrial and ribosomal counts and cell cycle phase) were evaluated and regressed out using a linear regression as implemented in Scanpy (scanpy.pp.regress_out). Furthermore, in order to integrate the datasets, the Harmony algorith is used (96). Then, a k-nearest neighbor graph was constructed based on Euclidean distance in principal component analysis space, considering a limited number of principal components. Finally, the Leiden algorithm was used to perform unsupervised clustering of cells (scanpy.tl.leiden).

Data visualization and identification of differential expression genes.

UMAP was used to visualize the data (97). The number of principal components used to calculate the embedding were the same as those used for the clustering. DEGs between "constriction" and "straight" cells were identified using scanpy.tl.rank_genes_groups implemented by Scanpy using the Wilcoxon test with tie correcction. In order to simplify the data exploration, original data are loaded into the BbrowserX platform using default parameters. Metadata generated by the Scanpy pipeline were added to BbrowserX easing the visualization.

Copy Number Alteration Inference.

Cells resulting from the filtering are used as input for the InferCNV pipeline v1.3.3 (Tickle T, Tirosh I, Georgescu C, Brown M, Haas B (2019). *inferCNV of the Trinity CTAT Project.*. Klarman Cell Observatory, Broad Institute of MIT and Harvard, Cambridge, MA, USA. https://github.com/broadinstitute/inferCNV) enabling the HMM model type 3, a cutoff of 0.1, disabling the cluster by goups, setting the analysis mode to "subclusters", performing the denoise and setting the reference group to the “straight” cells.

Gene Set Enrichment Analysis.

In order to evaluate pathways enriched in deregulated genes identified in the comparison constriction *vs* straight performed on the scRNA-seq data, a gene set enrichment analysis was carried out using the R package EnrichR that provides an interface to the EnrichR database (https://maayanlab.cloud/Enrichr/). The lists of genes upregulated (logFC>=0.1, pvalue <=0.05 and adjusted p-value <=0.05) and downregulated (logFC<=-0.1, p-value <=0.05 and adjusted p-value <=0.05) were used for an enrichment analysis performed on the Hallmark gene set available from the GSEA Molecular Signatures Database (https://www.gsea-msigdb.org/gsea/msigdb/genesets.jsp?collections).

S1.8 metaphase spreads of migrated cells.

U2OS cells were migrated in the micro-channel device designed for scRNA-seq and seeded on a 48-well plate, as previously described. Cells were maintained in culture to be seeded on round glass slides coated with fibronectin 10µg/ml in a 24-well plate. 4 days post trypsinization and collection from channels cells were processed for metaphase spreads on

slides ad described above. For this experiment 5 devices with straight channels and 10 devices with constrictions were used.

Carnoy's fixative solution: Methanol: Glacial acetic acid (3:1), prepare freshly and stored at -20 degrees. Hypotonic solution: 0.66g of KCL 3g of Na3Citrate in 500ml of water (RT).

S1.9 c-Myc Fluorescence in situ hybridization (FISH).

Slides with metaphase spreads were dehydrated in ethanol solution (70% EtOH 2 min, 85% EtOH 2 min, 100% EtOH 2 min). Slides were then air-dried and a probe mixture (2µl of probe and 8µl of buffer) was applied to each slide. Slides were sealed on bottom-slide glasses using dental gum to avoid evaporation of the probe mixture. Following addition of the probe mixture, slides were maintained in dark. Denaturation was performed placing the slides on the top of a pre-warmed thermo-block at 73˚C for 2 minutes. Hybridization was done incubating the slides overnight in 37˚C water-bath on the top of a thermo-block. Slides were then washed using WS1 and WS2 (prepared with NP-40 and SSC buffer 15557036, ThermoFisher) according to manufacture instructions, stained with DAPI and mounted using Mowiol.

Fig. S1

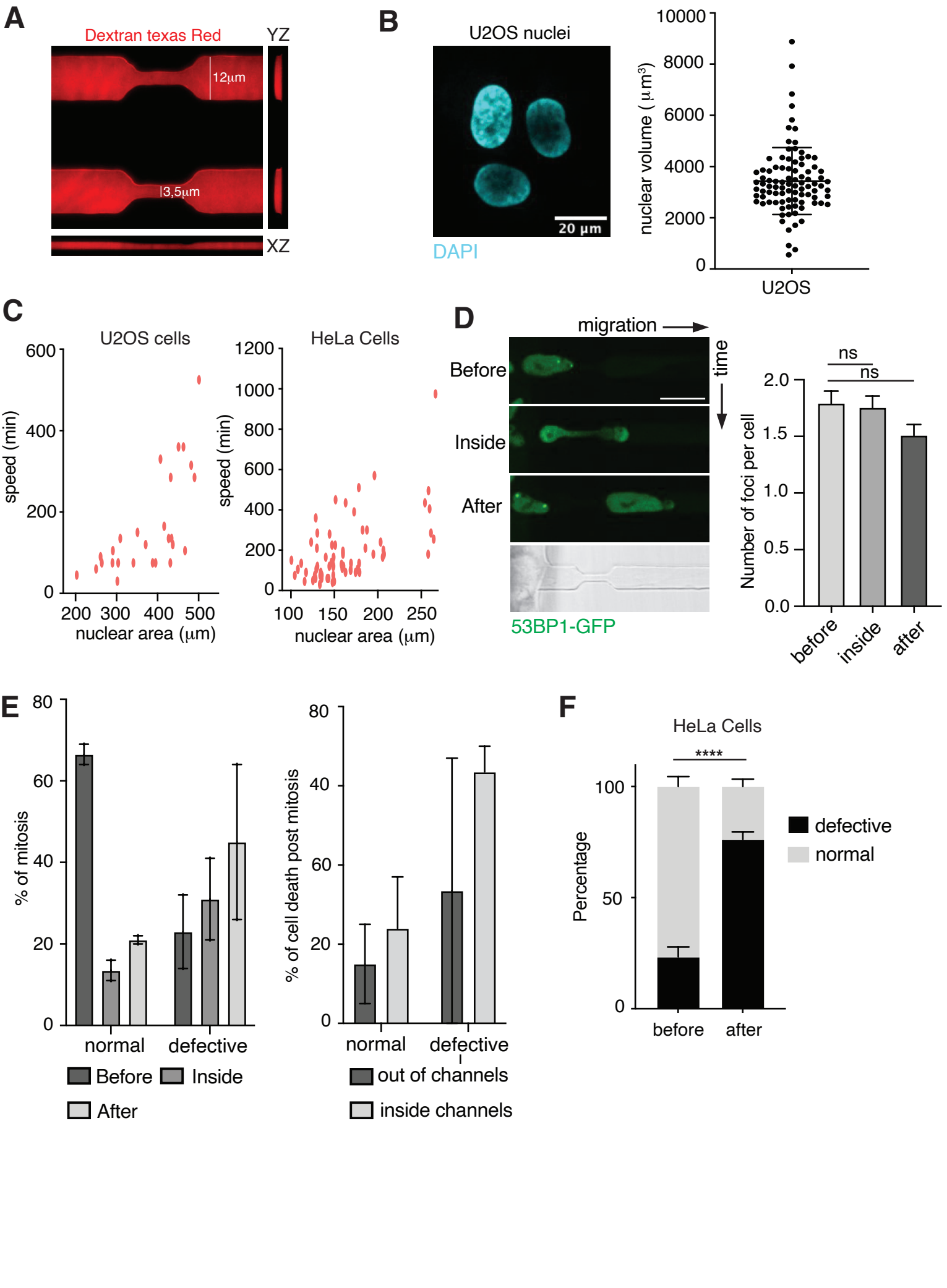
A
Dextran texas Red
YZ
12µm
3,5µm
XZ
B
U2OS nuclei
20 µm
DAPI
nuclear volume (µm³)
10000
8000
6000
4000
2000
0
U2OS
C
U2OS cells
HeLa Cells
speed (min)
nuclear area (µm)
D
migration
time
Before
Inside
After
53BP1-GFP
Number of foci per cell
ns
ns
before
inside
after
E
% of mitosis
normal
defective
Before
Inside
After
% of cell death post mitosis
out of channels
inside channels
F
HeLa Cells
****
Percentage
defective
normal
before
after

Fig. S1. Nuclear size influences interstitial migration, which in turn affects cell cycle progression and mitotic events in absence of DNA damage.

A) Immunofluorescence images of the micro-channels for interstitial migration assay with relative orthogonal projections showing channels and constriction sizes. Channels were filled with a 1mg/ml solution in PBS of Dextran Texas red 70.000 MW. Channels height is 6μm.

B) Analysis of nuclear volume in U2OS cells stained with DAPI using a custom-made macro designed in ImageJ. Representative images of DAPI staining (left) (scale bar: 20μm). Quantifications of nuclear volumes (right graph).

C) Time for passing a constriction during migration linearly correlates with nuclear size in U2OS and HeLa cells.

D) Time-lapse images of stable 53BP1-GFP U2OS cells migrating across constriction showing no increase of 53BP1-GFP foci while passing through the pore (left) and relative quantifications (right). Error bars are SEM and stats are calculated with one-way ANOVA. Scale bar: 20μm.

E) Increased defective mitoses in U2OS H2B-GFP Tubulin-mCherry migrating across constrictions correlates with increased cell death post mitosis. Error bars are SEM.

F) Analysis of H2B-mCherry HeLa cells show increase in mitotic defects in cells dividing inside of after constriction similarly to U2OS cells. ****=P value< 0.0001 two-way ANOVA.

Fig. S2

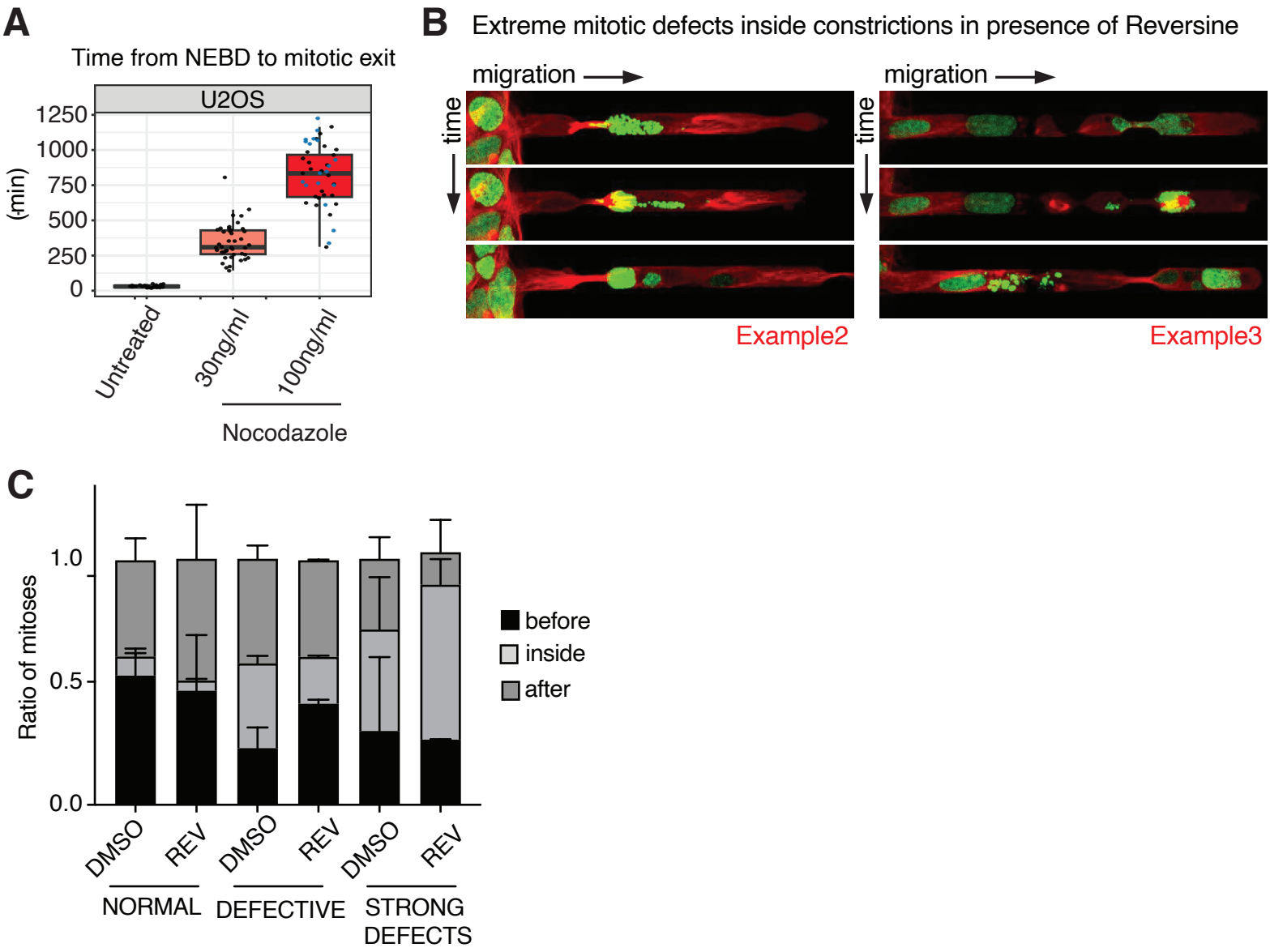

Fig. S2. Inhibition of SAC with Reversine synergizes with mechanical constraint during interstitial migration and leads to extreme mitotic defects.

A) SAC is functional in U2OS cells and delays mitotic progression following treatment with increasing doses of the anti-mitotic agent Nocodazole.

B) Representative examples of extreme mitotic defects caused by the combined action of mechanical stress during migration across constriction and SAC inhibition.

C) Quantifications of the ratio of defective and very defective mitoses according to channel position in presence or absence of Reversine. SAC inhibition increases the ratio of extreme mitotic defects inside constrictions. Error bars are SEM.

Fig. S3

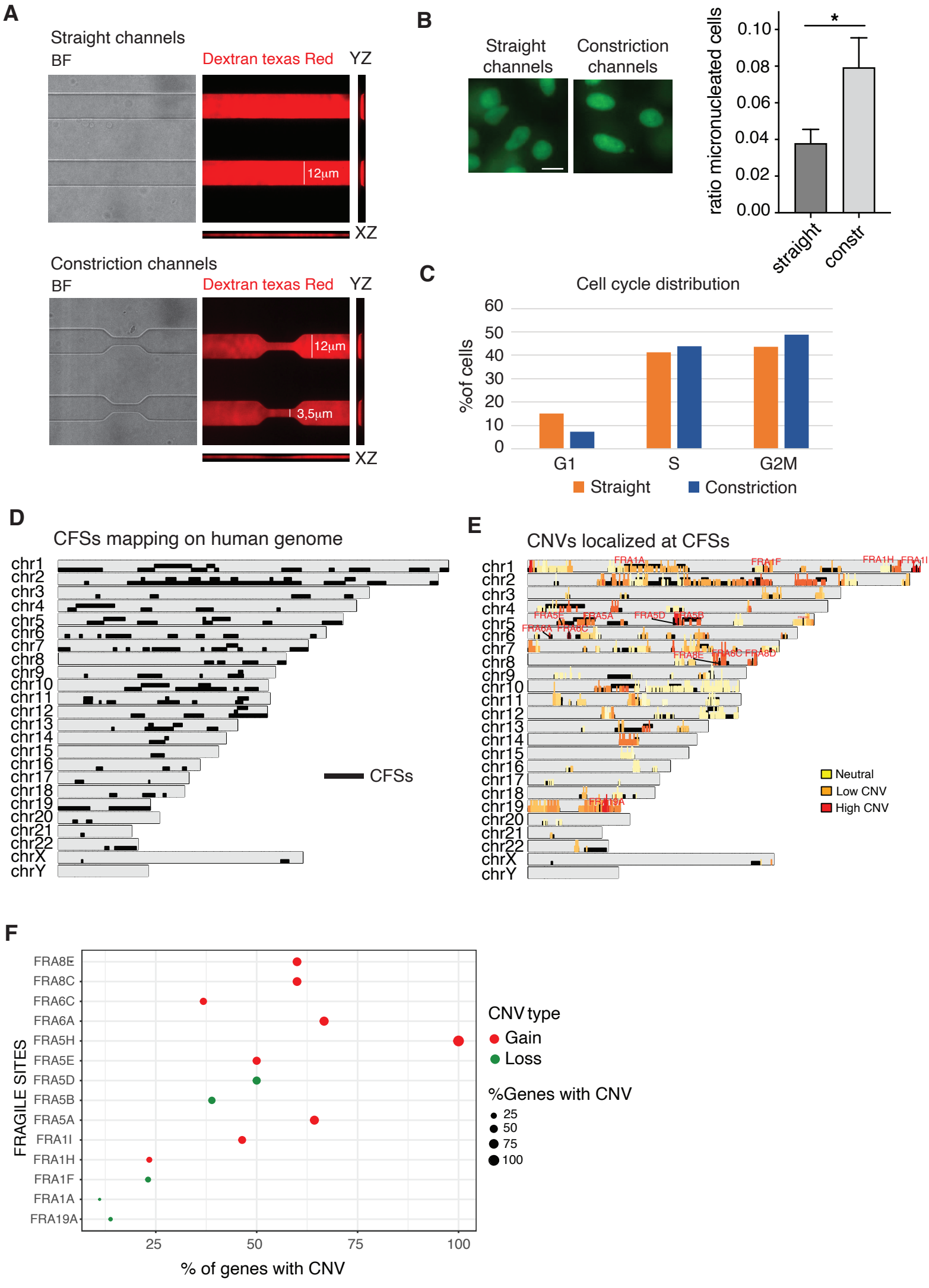
A
Straight channels
BF
Dextran texas Red
YZ
12µm
XZ
Constriction channels
BF
Dextran texas Red
YZ
12µm
3,5µm
XZ
B
Straight channels
Constriction channels
ratio micronucleated cells
0.10
0.08
0.06
0.04
0.02
0.00
*
straight
constr
C
Cell cycle distribution
%of cells
60
50
40
30
20
10
0
G1
S
G2M
Straight
Constriction
D
CFSs mapping on human genome
chr1
chr2
chr3
chr4
chr5
chr6
chr7
chr8
chr9
chr10
chr11
chr12
chr13
chr14
chr15
chr16
chr17
chr18
chr19
chr20
chr21
chr22
chrX
chrY
CFSs
E
CNVs localized at CFSs
FRA1A
FRA1F
FRA1H
FRA1I
FRA5E
FRA5A
FRA5D
FRA5B
FRA8A
FRA8C
FRA8E
FRA8C
FRA8D
FRA19A
Neutral
Low CNV
High CNV
F
FRAGILE SITES
FRA8E
FRA8C
FRA6C
FRA6A
FRA5H
FRA5E
FRA5D
FRA5B
FRA5A
FRA1I
FRA1H
FRA1F
FRA1A
FRA19A
25
50
75
100
% of genes with CNV
CNV type
Gain
Loss
%Genes with CNV
25
50
75
100

Fig.S3. Interstitial migration across one single constriction increases micronuclei and induces CNVs at specific CFSs.

A) Bright-field and immunofluorescence images of straight and constriction channels of the custom-made device for interstitial migration and single-cell RNAseq with relative orthogonal projections, channels and constriction sizes. Channels were filled with a 1mg/ml solution in PBS of Dextran Texas red 70.000 MW. Channels height is 6μm.

B) U2OS H2B-GFP cells migrated in the device with straight or constriction channels show increased number of micro nucleated cells following migration across constriction. *=P value< 0.05 unpaired t-test, error bars are SEM. Scale bar: 20μm.

C) Cell cycle distribution of U2OS cells migrated across straight or constriction channels and analyzed by single-cell RNAseq.

D) Graphical representation mapping the CFSs (black bars) on the human chromosomes (CFSs were identified using HumCFS database (1)).

Fig. S4

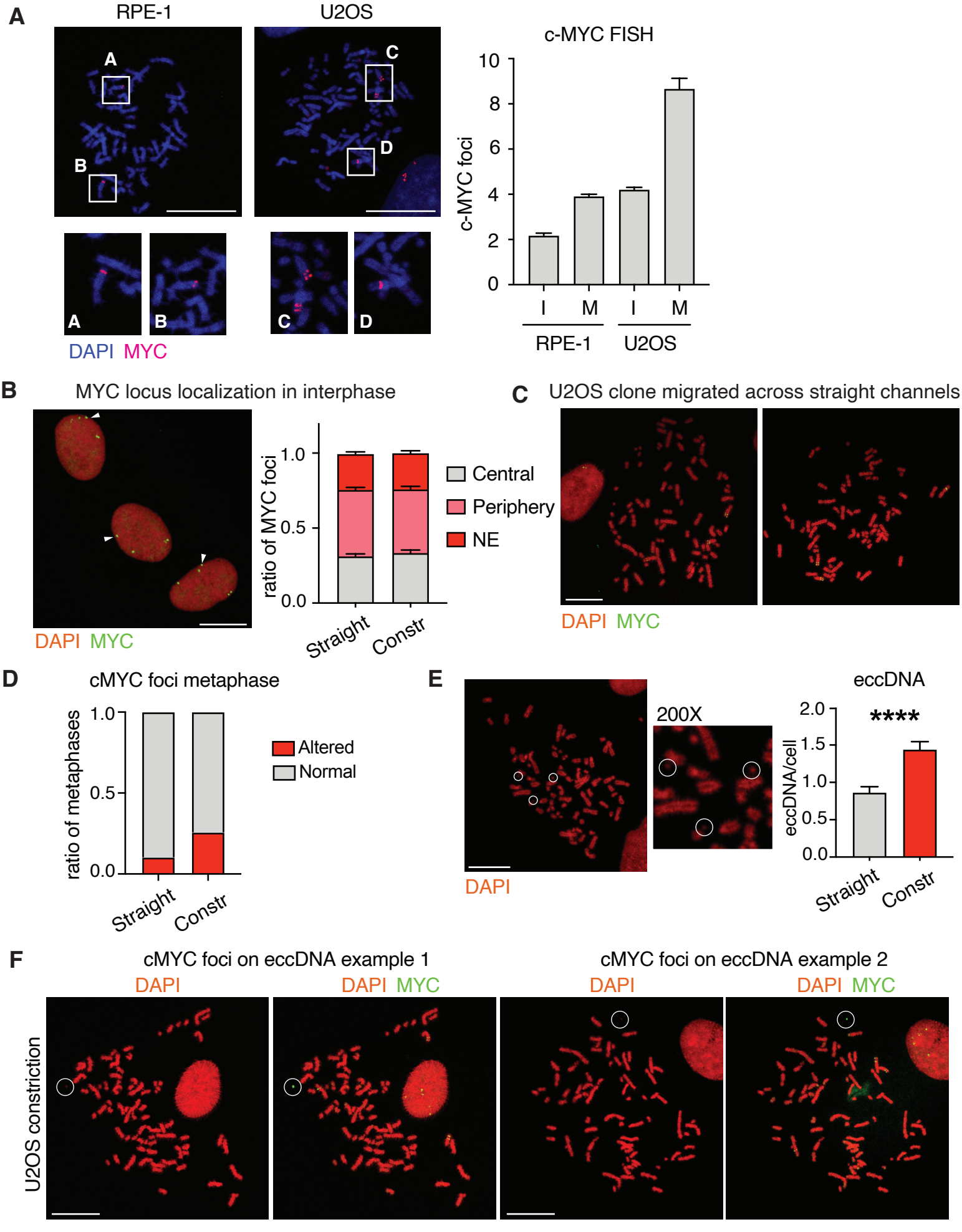
A
RPE-1
U2OS
A
B
C
D
DAPI MYC
c-MYC FISH
c-MYC foci
10
8
6
4
2
0
I
M
I
M
RPE-1
U2OS
B
MYC locus localization in interphase
DAPI MYC
ratio of MYC foci
1.0
0.5
0.0
Straight
Constr
Central
Periphery
NE
C
U2OS clone migrated across straight channels
DAPI MYC
D
cMYC foci metaphase
ratio of metaphases
1.0
0.5
0.0
Straight
Constr
Altered
Normal
E
DAPI
200X
eccDNA
eccDNA/cell
2.0
1.5
1.0
0.5
0.0
****
Straight
Constr
F
cMYC foci on eccDNA example 1
cMYC foci on eccDNA example 2
DAPI
DAPI MYC
DAPI
DAPI MYC
U2OS constriction

Fig.S4. c-MYC locus localizes at the nuclear periphery in U2OS cells during interphase and it is prone to amplifications following interstitial migration.

A) Immunofluorescence images showing the validation of c-MYC FISH probe on metaphase spreads from diploid immortalized non-transformed RPE-1 cells (left) and the representative c-MYC locus configuration in the U2OS clone used for the scRNA-seq experiments (right) Scale bars: 20μm. Bar-plot graph shows the average number of c-MYC foci in RPE-1 and U2OS cells during interphase (I) or metaphase (M). Error bars are SEM.

B) FISH immunofluorescence image showing c-MYC locus at the nuclear periphery and near the nuclear envelope in U2OS during interphase (left) with relative quantifications (right). White arrowheads highlight c-MYC at the nuclear envelope. Scale bar: 20μm. Error bars are SEM.

C) Representative FISH examples of the regular c-MYC locus configuration in the U2OS clone migrated across straight channels. Scale bar: 20μm.

D) Quantifications of the fraction of metaphase spreads with altered c-MYC locus configuration in U2OS cells migrated across straight channels and channels with constrictions.

E) Representative immunofluorescence image (with 200X magnification) of U2OS metaphase spread carrying eccDNA molecules stained with DAPI (highlighted by white circles) Scale bar: 20μm. The bar-plot graph shows the quantifications of eccDNA molecules per metaphase in U2OS cells migrated in straight or constriction channels. ****=P value< 0.0001 unpaired t-test, error bars are SEM.

F) Immunofluorescences showing rare examples of c-MYC FISH signal colocalizing on eccDNA molecules in metaphase spreads of U2OS migrated across constrictions. Scale bars: 20µm.

Fig. S5

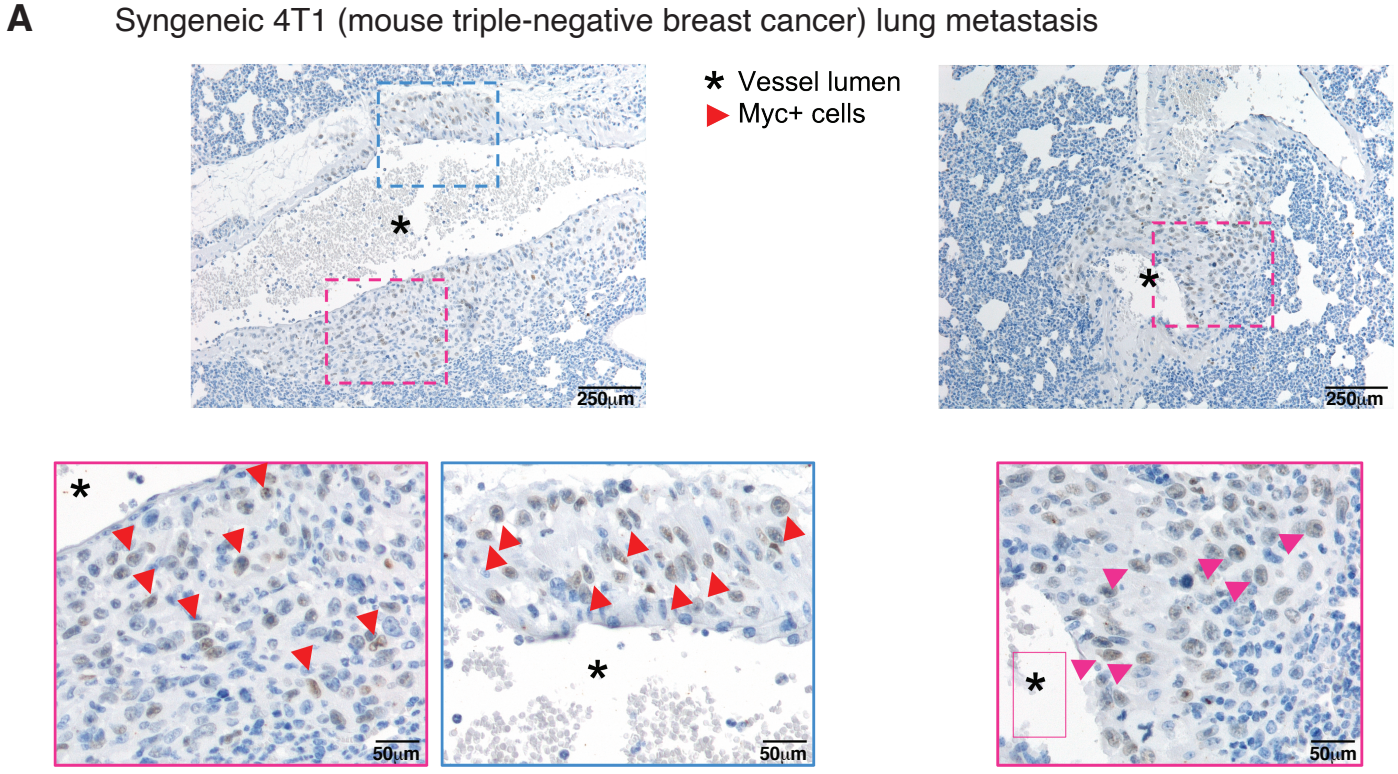

Fig.S5. Metastasis leads to c-MYC protein expression heterogeneity in tumor cells.

A) Immunohistochemistry images of lung metastasis derived from a syngeneic model of human TNBC stained for c-MYC. 4T1 cells metastasized in the lungs show increased heterogeneity for c-MYC protein expression.

SI References

1. R. Kumar *et al.*, HumCFS: a database of fragile sites in human chromosomes. *BMC Genomics* **19**, 985 (2019).